A dynastic elite in monumental Neolithic society

A dynastic elite in monumental Neolithic society

Author list

Lara M. Cassidy[1], Ros Ó Maoldúin[1,2,3], Thomas Kador[4], Ann Lynch[5], Carleton Jones[6], Peter C. Woodman[†,7], Eileen Murphy[8], Greer Ramsey[9], Marion Dowd[10], Alice Noonan[1], Ciarán Campbell[1], Eppie R. Jones[1,11], Valeria Mattiangeli[1] and Daniel G. Bradley[1]

Affiliations:

[1] Smurfit Institute of Genetics, Trinity College Dublin, Dublin 2, Ireland

[2] The Irish Fieldschool of Prehistoric Archaeology, National University of Ireland, Galway, Ireland

[3] Archaeological Management Solutions, Consultancy, Kilrush, Clare, Ireland

[4] UCL Arts and Sciences, University College London, London, WC1E 6BT, UK

[5] Former Chief Archaeologist, National Monuments Service, Department of Culture, Heritage and the Gaeltacht, Custom House, Dublin

[6] School of Geography and Archaeology, National University of Ireland Galway, Galway, Ireland

[7] Department of Archaeology, University College Cork, Cork, Ireland

[8] Archaeology & Palaeoecology, School of Natural & Built Environment, Queen's University Belfast, Belfast BT7 1NN, Northern Ireland

[9] National Museums NI, Cultra, Holywood BT18 0EU, Northern Ireland

[10]CERIS, School of Science, Institute of Technology Sligo, Sligo, Ireland

[11] Department of Zoology, University of Cambridge, Downing Street, Cambridge CB2 3EJ, UK

[†] Deceased

The nature and distribution of political power in Neolithic Europe remains poorly understood[1]. During the period, many societies began to invest heavily in monument-building, suggesting an increase in social organisation. The scale and sophistication of megalithic architecture along the Atlantic seaboard is particularly impressive, culminating in the great passage tomb complexes[2]. While megalith builders have often been proposed as co-operative networks of independent communities, the human expenditure required for the largest monuments has led some to emphasize hierarchy[3], the most extreme case being a small elite marshalling the labour of masses. Here we present evidence that such a social stratum was established during the Irish Neolithic period. In a sampling of 44 whole genomes, we identify the adult son of a first-degree incestuous union discovered within the most elaborate recess of the imposing Newgrange passage tomb. Socially sanctioned matings of this nature are highly rare and occur almost exclusively among politico-religious elites[4], specifically within polygynous and patrilineal royal families headed by god-kings[5,6]. We identify relatives of this individual within two other major passage tomb complexes 150km to the west, as well as dietary differences and unprecedented fine-scale haplotypic structure between passage tomb samples and the larger population, implying hierarchy. This system emerged against a backdrop of rapid maritime colonisation that displaced a unique Mesolithic isolate, although Irish hunter-gatherer introgression is detected within the Neolithic population.

Ancient genomes have demonstrated common ancestry between the societies of the Atlantic Neolithic[7–9], while recent modelling has defined repeat expansions of megalithic architecture from northwest France, at a pace implying more advanced maritime technology than previously assumed in these regions[10]. This includes the spread of passage tombs along the Atlantic façade during the 4th millennium BC, a period which also saw the arrival of agriculture to Ireland alongside other distinct megalithic traditions. These structures reached one of their highest known concentrations and diversities on the island. However the political systems underlying these societies remain obscure, as does the genetic input from indigenous Mesolithic hunter-gatherers.

To investigate, we shotgun sequenced individuals from the Irish Mesolithic (n=2) and Neolithic (n=42) to a median 1.14X coverage (Fig. 1a, Supplementary Tables 1, 2). We imputed 43 of these alongside relevant ancient genomes (Supplementary Table 3), including an additional 20 British and Irish individuals[7,9,11]. These were merged with a published imputed ancient dataset[12] to allow for finescale haplotypic inference of population structure[13] and estimation of inbreeding. Four key individuals were subsequently sequenced to higher (13-20X) coverage.

All major Irish Neolithic funerary traditions were sampled: court tombs, portal tombs, passage tombs, Linkardstown-type burials and natural sites (Fig. 1a, c; Supplementary Information section 1). Within this, the earliest Neolithic human remains from the island, interred at Poulnabrone portal tomb[14], are of majority *Early_Farmer* ancestry and show no evidence of inbreeding (Extended Data Fig. 1; Fig. 1a), implying that from the very outset agriculture was accompanied by large-scale maritime colonisations. ADMIXTURE and ChromoPainter analyses do not distinguish between the Irish and British Neolithic populations and confirm[7,8] the Spanish Early Neolithic as the best proxy source of their *Early_Farmer* ancestry (Fig. 1d, Extended Data Figs. 1, 2), emphasising the importance of Atlantic and Mediterranean waterways in their forebearers' expansions.

Overall, no increase in inbreeding is seen through time in Neolithic Ireland, indicating that communities maintained sufficient size and communication to avoid matings of 5th degree relatives or closer (Fig. 1a). However, we report a single extreme outlier interred within Newgrange passage tomb, a focal point of the UNESCO monumental landscape of Brú na Bóinne (Fig. 2a). Incorporating over 200,000 tonnes of earth and stone, this megalithic mound is one of the most spectacular of its

kind in Europe[15]. While externally designed for public consumption, internally, the tomb consists of a single narrow passage with a specialised ritual inventory, whose winter solstice solar alignment would have been viewed only by a select few. Unburnt, disarticulated human bone was found concentrated within the most elaborately decorated recess of the terminal cruciform chamber, including the cranial remains of an adult male (NG10; Fig. 2b; Supplementary Information 1.4.1). This exceptional location is matched by an unprecedented genomic heritage. He possessed multiple long runs of homozygosity (ROH), each comprising large fractions of individual chromosomes (Fig. 2e; Extended Data Fig. 3a), and totalling to a quarter of the genome (Inbreeding Coefficient = 0.25). This marks him as the offspring of a first order incestuous union, a near universal taboo for entwined biological and cultural reasons[4]. However, given the auspicious nature of the interment, his parentage was very likely socially sanctioned.

While simulations cannot distinguish whether his parents were full siblings or parent and offspring (Extended Data Fig. 3), the only definitive acceptances of such matings occur among siblings, specifically within polygynous elites, as part of a rarely observed phenomenon known as "royal" or "dynastic" incest[4,6,16]. In all documented cases (e.g. Hawaii, Inca Empire, Ancient Egypt), this behaviour co-occurs with the deification of political leaders and is typically limited to ruling families, whose perceived divinity exempts them from social convention. Both full and half-sibling marriages are found most commonly in complex chiefdoms and early states, being generally viewed as a means to intensify hierarchy and legitimise power in the absence of more advanced bureaucratic systems, alongside tactics such as extravagant monumentalism and public ritual[17,18,19]. We propose a comparable set of social dynamics was in operation in Ireland by the Middle Neolithic, and, given the construction of solstice-aligned passage tombs similar to Newgrange in Wales, Orkney and Brittany[20], may have occurred outside the island as well. Notably, levels of consanguinity are consistently low and decrease through time across our wider ancient dataset (Extended Data Fig. 4), with only one other incidence of close inbreeding detected, the son of 2nd-3rd degree relatives from a Swedish megalith[9].

The Brú na Bóinne passage tombs appear in Medieval mythology, which relates their construction to magical manipulations of the solar cycle by a tribe of gods, leading to unresolved

speculation about the durability of oral tradition across millennia[21]. Such longevity seems unlikely but, surprisingly, our results strongly resonate with mythology first recorded in the 11th century AD, which has a builder-king copulate with his sister to restart the daily solar cycle[22]. A Middle Irish placename for the Dowth passage tomb which neighbours Newgrange, *Fertae Chuile,* is based on this lore and can be translated as "Hill of Sin" or "Hill of Incest"[22,23].

A second centre of the passage tomb tradition is found 150km west near the Atlantic coast. Here, the mega-cemeteries of Carrowmore and Carrowkeel have origins pre-dating the construction of Newgrange by several centuries, with depositions at Carrowkeel continuing until at least the end of the Neolithic[24]. Using both SNP- and haplotype-sharing analyses, we uncover a web of relatedness connecting these sites to both Newgrange and the atypical Millin Bay megalith on the northeast coast, recognised as part of the passage tradition for its artwork and morphological features.

Firstly, using lcMLkin[25] (Fig. 2c), we find the earliest passage tomb genome in the dataset (car004[9]), interred within the focal monument at Carrowmore, has detectable distant kinship with NG10, as well as with other later individuals from Carrowkeel and Millin Bay (CAK533 and MB6). A similar kinship coefficient (≥6th degree) is also seen between NG10 and CAK532 (Extended Data Fig. 5a), demonstrating familial ties between several of the largest hubs of the tradition.

Secondly, in a fineSTRUCTURE[13] analysis of Atlantic Neolithic genomes, samples from Newgrange, Carrowkeel and Millin Bay form a distinct cluster, which is split from a larger British and Irish grouping (Fig. 1d, e). The robustness of this cluster is confirmed using a larger ancient dataset (Extended Data Fig. 2). ChromoPainter[13] also identifies excessive reciprocal haplotype donation specifically between NG10 and CAK532, confirming their kinship (Extended Data Fig. 5b). Evidence of more distant relatedness is seen between the inferred relatives of car004[9], who share elongated haplotypic chunks with one another; this signature of recent shared ancestry also links CAK530 to CAK533 and NG10 (Fig. 2d; labelled on Fig. 1d).

The earlier car004[9] genome is of low coverage (0.04X) and thus was excluded from ChromoPainter analysis. However, *D*-statistics demonstrate that this sample preferentially forms a clade with the passage cluster ($Z > 3.4$; Supplementary Table 10), despite being closer in time to the majority of samples from the larger British-Irish cluster. Moreover, this attraction is only partially

driven by the aforementioned kin connections, which we further corroborate. Downsampling tests on the larger dataset demonstrate *D*-statistic results for car004 to be highly significant (Supplementary Table 11).

Taken together, we favour that the haplotypic structure within our dataset is driven by excessive IBD sharing between passage tomb samples, implying non-random mating across large territories of the island. A high degree of social complexity would be required to achieve this, as is predicted by the parentage of NG10. However, our non-passage tomb genomes are largely earlier in date and denser sampling of diverse sites from the Late Neolithic will be required to evaluate the contribution of temporal drift to the fineSTRUCTURE clustering. Stable isotope values also differentiate passage tomb interments (Fig. 1b). Their combination of high $\delta^{15}N$ and depleted $\delta^{13}C$ values is best explained by a more privileged diet of meat and animal products, although it remains to be seen how this relates to broader dietary change during the period.

Simpler court and portal tombs lack the artwork and prestigious grave-goods of the passage tradition, and are arguably a manifestation of smaller lineage-based societies[3]. These architectures do not typically occur within passage tomb cemeteries, although exceptions exist, including a court tomb constructed beside Carrowmore, which showed a potential instance of inter-site kinship[9]. We find evidence of both distant kinship (Supplementary Information section 6.5) and societal structure between another pair of distinct but neighbouring megaliths (10 km apart) - Poulnabrone portal tomb[14] and Parknabinnia court tomb[26]. Their majority male cohorts show a significant difference in the frequency of two Y chromosome haplogroups (P=0.035, Fisher exact test), as well as dietary difference (Fig. 1b, Extended Data Figs. 6). Given the lack of close kin within either tomb, we exclude small family groups as their sole proprietors and interpret our results as the result of broader social differentiation with an emphasis on patrilineal descent. The double occurrence of a rare Y haplogroup (H2a) among the individualised male Linkardstown burials of the southeast provides further evidence of the importance of patrilineal ancestry in these societies[9], as does the predominance of a single Y haplogroup (I-M284) across the Irish and British Neolithic (Extended Data Fig. 7).

It is hypothesised that the spread of agriculture into Britain and Ireland was assisted by pre-existing Mesolithic maritime connections[27]. However, our results suggest that prior to the Neolithic

the Irish Sea posed a formidable barrier to gene flow. Irish hunter-gatherer (HG) genomes form a distinct cluster within a wider grouping of Mesolithic HGs from northwest Europe[11,28], sharing excessive levels of drift with each other despite over half a millennium's separation (Fig. 3a, Extended Data Fig. 2, Supplementary Information section 4). In contrast, British HGs show no differentiation from continental contemporaries[11]. This accords with paleogeographic models positing a Doggerland bridge between Britain and the continent for most of the Mesolithic, but a pre-Holocene separation of Ireland[29].

Irish HGs also exhibit the largest degree of short ROH (Fig. 3b) yet described in any ancient, or indeed modern genome, a signature of ancestral constriction that supports a prolonged island isolation. This implies that continental and British HGs lacked the technology or impetus required to maintain frequent contact with Ireland and reflects the relatively late Mesolithic colonisation of the island, followed by a sharp divergence in lithic assemblages[30]. Nonetheless, with no signatures of recent inbreeding (Fig. 1a), it appears Irish HGs were capable of sustaining outbreeding networks within the island itself, despite an estimated carrying capacity of only 3,000-10,000 individuals[30].

Ultimately, Irish HGs originate from sources related to Italian Upper Palaeolithic individuals[28] (Fig. 3a), with no evidence of contribution from an earlier western lineage that persisted in Spain[31]. However, we detect a significant excess of this ancestry in the Luxembourg Mesolithic relative to Irish and British HGs (Supplementary Table 9), demonstrating its survival outside Iberia. We also explore the genetic legacy of Irish HGs in the island's Neolithic population and discover an incidence of direct ancestral contribution. Within a broader pattern of high haplotypic affinities among European farmers to local HG groups (Fig. 3c), we uncover an outlier from Parknabinnia (PB675) with a disproportionate and specifically Irish HG contribution. High variance in HG ancestry across the genome and an excess of elongated Irish HG haplotypes support a recent introgression (Extended Data Fig. 8), estimated within four generations (Supplementary Information section 3).

This finding, taken together with evidence of local HG input into the Scottish Neolithic[11], implies recurring interactions between incoming farmers and the indigenous populations of the islands. Notably, a ~4th degree relative of PB675 was interred within the same tomb (Extended Data Fig. 5a), implying this outlier was integrated within the community. An alternate instance of diversity

in those selected for megalithic interment is seen in a male infant from Poulnabrone (PN07) with a dietary signature of breastfeeding (Fig. 1b, Extended Data Fig. 6). This individual has a clear trisomy of chromosome 21, the earliest definitive discovery of a case of Down syndrome[32].

Overall, our results demonstrate the capacity of ancient genomes to shed light not only on population movements, but on political systems and social values where no written records exist. This is particularly true when imputation and haplotypic analyses are utilised, which we affirm outperform popular SNP-based methods in the resolution of ancient population structure (Extended Data Fig 9). Together with estimations of inbreeding and kinship, these methods broaden the scope within which we can study the development of agricultural societies from chiefdoms to civilisations. Specifically, our findings support a re-evaluation of social stratification and political integration in the megalithic cultures of the Atlantic[10], with the passage tomb building societies of Ireland possessing several attributes found within early states and their precursors.

References

1. Hinz M., Müller J., Wunderlich M. The monumentalisation of European landscapes. in *Megaliths, Societies, Landscapes: Early Monumentality and Social Di erentiation in Neolithic Europe* (ed. Hinz M., Müller J., Wunderlich M.) vol. 1 21–23 (Habelt, 2019).
2. Cunliffe, B. *Facing the Ocean: the Atlantic and its Peoples*. (Oxford University Press, 2004).
3. Burenhult, G. Megalithic Symbolism in Ireland and Scandinavia in light of new evidence from Carrowmore. *Perspectiva em Diálogo* (1999).
4. Wolf, A. P. *Incest Avoidance and the Incest Taboos: Two Aspects of Human Nature*. (Stanford University Press, 2014).
5. Goggin, J. M. & Sturtevant, W. P. The Calusa: A Stratified, Nonagricultural Society (With Notes on Sibling Marriage). in *Explorations in Cultural Anthropology. Essays in Honour of George Peter Murdock* (ed. Goodenough, W. H.) 179–219 (McGraw-Hill, 1964).
6. van den Berghe, P. L. & Mesher, G. M. Royal incest: a reply to Sturtevant. *Am. Ethnol.* **8**, 187–188 (1981).
7. Cassidy, L. M. *et al.* Neolithic and Bronze Age migration to Ireland and establishment of the insular Atlantic genome. *Proc. Natl. Acad. Sci. U. S. A.* **113**, 368–373 (2016).
8. Olalde, I. *et al.* The Beaker phenomenon and the genomic transformation of northwest Europe. *Nature* **555**, 190–196 (2018).
9. Sánchez-Quinto, F. *et al.* Megalithic tombs in western and northern Neolithic Europe were linked to a kindred society. *Proc. Natl. Acad. Sci. U. S. A.* **116**, 9469–9474 (2019).
10. Paulsson, B. S. Radiocarbon dates and Bayesian modeling support maritime diffusion model for megaliths in Europe. *Proc. Natl. Acad. Sci. U. S. A*. **116**, 3460–3465 (2019).
11. Brace, S. *et al.* Ancient genomes indicate population replacement in Early Neolithic Britain. *Nat Ecol Evol* **3**, 765–771 (2019).
12. Martiniano, R. *et al.* The population genomics of archaeological transition in west Iberia: Investigation of ancient substructure using imputation and haplotype-based methods. *PLoS Genet.* **13**, e1006852 (2017).

13. Lawson, D. J., Hellenthal, G., Myers, S. & Falush, D. Inference of population structure using dense haplotype data. *PLoS Genet.* **8**, e1002453 (2012).
14. Lynch, A. *Poulnabrone: An Early Neolithic Portal Tomb in Ireland*. (Stationery Office, 2014).
15. O'Kelly, M. J. *Newgrange*. (Thames and Hudson, 1983).
16. Huebner, S. R. 'Brother-Sister' Marriage in Roman Egypt: a Curiosity of Humankind or a Widespread Family Strategy? *The Journal of Roman Studies* **97**, 21–49 (2007).
17. Kolb, M. J. *et al.* Monumentality and the Rise of Religious Authority in Precontact Hawai'i [and Comments and Reply]. *Curr. Anthropol.* **35**, 521–547 (1994).
18. Gates, H. Refining the Incest Taboo: With Considerable Help from Bronislaw Malinowski. in *Inbreeding, Incest, and the Incest Taboo: The State of Knowledge at the Turn of the Century* (eds. Wolf, A. P. & Durham, W. H.) 139–160 (Stanford University Press, 2005).
19. Kirch, P. V. *How Chiefs Became Kings: Divine Kingship and the Rise of Archaic States in Ancient Hawai'i*. (University of California Press, 2010).
20. Hensey, R. *First Light: The Origins of Newgrange*. (Oxbow Books, 2015).
21. Hensey, R. Rediscovering the Winter Solstice Alignment at Newgrange, Ireland. in *The Oxford Handbook of Light in Archaeology* (ed. Papadopoulos C. and Moyes H.) (Oxford University Press, 2017).
22. Carey, J. Time, Memory, and the Boyne Necropolis. *Proc. of the Harvard Celtic Colloquium* **10**, 24–36 (1990).
23. Gwynn, E. *The metrical Dindshenchas. 4. Text, translation, and commentary*. (School of Celtic Studies, Dublin Institute for Advanced Studies, 1991).
24. Kador, T. *et al.* Rites of Passage: Mortuary Practice, Population Dynamics, and Chronology at the Carrowkeel Passage Tomb Complex, Co. Sligo, Ireland. *Proc. of the Prehist. Soc.* **84**, 225–255 (2018).
25. Lipatov, M., Sanjeev, K., Patro, R. & Veeramah, K. Maximum Likelihood Estimation of Biological Relatedness from Low Coverage Sequencing Data. *bioRxiv* 023374 (2015)
26. Jones, C. The north Munster atypical court tombs of western Ireland – social dynamics, regional trajectories and responses to distant events over the course of the Neolithic. in *Megaliths* -

Societies - Landscapes. Early Monumentality and Social Differentiation in Neolithic Europe (ed. Müller, J. Hinz, M., Wunderlich, M.) 979–1000 (Habelt Verlag, 2019).

27. Garrow, D. & Sturt, F. Grey waters bright with Neolithic argonauts? Maritime connections and the Mesolithic--Neolithic transition within the 'western seaways' of Britain, c. 5000--3500 BC. *Antiquity* **85**, 59–72 (2011).
28. Fu, Q. *et al.* The genetic history of Ice Age Europe. *Nature* **534**, 200–205 (2016).
29. Brooks, A. J., Bradley, S. L., Edwards, R. J. & Goodwyn, N. The palaeogeography of Northwest Europe during the last 20,000 years. *J. Maps* **7**, 573–587 (2011).
30. Woodman, P. *Ireland's First Settlers: Time and the Mesolithic.* (Oxbow Books, 2015).
31. Villalba-Mouco, V. *et al.* Survival of Late Pleistocene Hunter-Gatherer Ancestry in the Iberian Peninsula. *Curr. Biol.* **29**, 1169–1177.e7 (2019).
32. Rivollat, M., Castex, D., Hauret, L. & Tillier, A.-M. Ancient Down syndrome: An osteological case from Saint-Jean-des-Vignes, northeastern France, from the 5-6th century AD. *Int J Paleopathol* **7**, 8–14 (2014).

Fig. 1. Fine-scale haplotypic and dietary structure in the Neolithic. a, Timeline of analysed Irish genomes with inbreeding coefficients shown for those of sufficient coverage. All dates are direct excluding CAK534 (translucent). Sample site key follows panel **c**. The earliest widespread evidence of Neolithic activity (cereal/house horizon) is marked with a black line. The Irish Neolithic ends *circa* 2500 BC. **b,** Stable isotope values for Irish and British Neolithic samples (n=292). Irish sample key follows **c,** with those included in aDNA analysis outlined in black. British samples are shown as hollow shapes - Scotland: black, England/Wales: grey; circles: pre-3400 BC, squares: post-3400 BC. A high-trophic-level infant with Down syndrome is labelled. **c,** Site locations for Irish individuals sampled or included in this study coloured by burial type - court tomb (yellow), portal tomb (blue), Linkardstown-type (green), passage and related (magenta), natural sites (light pink) and the unclassified Ballynahatty[7] megalith (light blue). Sites outlined in black were included in aDNA analysis. **d,** ChromoPainter[13] PCA of Atlantic Neolithic genomes (n=57) generated using a matrix of haplotypic length-sharing. Passage tomb outliers in Fig. 2d are labelled. **e,** fineSTRUCTURE dendrogram derived from the same matrix with five consistent clusters.

Fig. 2. Genomic signals of dynasty among focal passage tomb interments. a, Front elevation and interior of Newgrange passage tomb (photo credits: Fáilte Ireland; Photographic Unit, National Monuments Service) **b,** Plan of chamber after O'Kelly 1983. **c,** The coefficient of relatedness (Pi-Hat) between another auspicious interment from the central monument at Carrowmore, car004[9], and 38 British and Irish Neolithic samples, with the top five hits labelled (CAK68 and CAK530 are equal in value). **d,** Average length of donated haplotypic chunks between all reciprocal pairs of the 'passage cluster' (pink; n=42) and 'British-Irish cluster' (grey; n=1190) as defined by fineSTRUCTURE in Fig. 1e. Highest values for passage cluster pairs are marked along the x-axis, with an excess of longer chunks shared between the inferred kin of car004 (CAK533, MB6, NG10) in **c**. Darker lines link reciprocal donations. Combined symbols are used for inter-site pairs. **e,** A sliding window of heterozygosity is plotted for transversions along selected chromosomes of NG10, revealing extreme ROH.

Fig. 3. Origins and Legacy of the Irish Mesolithic. a, Estimates of shared drift between Irish and British/continental HGs (jittered) from the Mesolithic and Upper Paleolithic (triangles: Magdalenian culture). Top ten hits with sufficient coverage are cross-compared in a heatmap. **b,** Short and long ROH spectra in modern and ancient genomes. Hollow shapes indicate direct (rather than imputed) diploid calls. For four Irish samples both imputed and direct data are presented, showing close agreement. **c,** Normalised haplotypic length donations from HG populations to Neolithic individuals, arranged by their geographic region (labelled). The top three HG donors are outlined for each individual. Donor population colour key follows that in panel **b**, with British and Northwestern HGs merged into one donor population (blue).

Methods

Sampling and Sequencing

We sampled 54 petrous temporal bones and 12 teeth (Supplementary Table 1) sourced from 20 archaeological sites (Supplementary Information section 1). Two of these, PN10 and PN113, were later found to belong to the same individual. Processing was carried out in clean-room facilities dedicated to ancient DNA research at Trinity College Dublin. Photographs were taken prior to sample alteration and these are available upon request to the authors. The dense otic capsule region of petrous bones and the root cementum of teeth were targeted for sampling. Bone/tooth powder (130-150mg) was subject to a described silica-column method[33] of DNA extraction with modifications[34]. Three successive extractions were performed on samples (incubation times of 24 hours at 37°C). Five samples were subject to a modified protocol, with powder first washed twice with EDTA (0.5M) and then subject to a single extraction (incubation time of 48 hours at 37°C).

Select sample extracts, typically the 3rd, were purified at a volume of 55µl and NGS double-stranded libraries were created from 16.50µl aliquots, following previously described methods[7,35] that are based on established protocol[36]. Library amplification reactions were carried out using Accuprime Pfx Supermix (Life Technology), primer IS4 (0.2µM), a specific indexing primer (0.2µM) and 3µl of library as previously described[7], and DNA concentrations assessed on an Agilent 2100 Bioanalyzer. Amplified libraries were first screened for endogenous human content on an Illumina MiSeq platform (TrinSeq, Trinity College Dublin) using 65 or 70 bp single-end sequencing. Extracts with sufficient human endogenous content (>5%) and concentration (>0.5 ng/µl at 12 PCR cycles) were incubated with USER Enzyme (volume of 5µl to 16.50µl of extract) for 3 hours at 37°C, to repair post-mortem molecular damage. Following this, library creation and amplification was carried out as described above. USER-treated libraries from a total of 45 individuals were sent for higher coverage sequencing at Macrogen Inc., Seoul, Korea (100 bp single-end with the exception of JP14, for which 100bp paired-end data was also obtained). Detailed experimental and sequencing results are found in Supplementary Table 2.

Demultiplexed data returned in FASTQ format were subject to quality control using the FastQC suite[37]. Residual adapter sequences were trimmed using cutadapt v1.2.1[38], with non-default parameters *-m 34* and *-O 1*. Quality trimming was performed on read ends where necessary. Paired-end reads from JP14 were merged and trimmed for adapters using the leeHom software [39]. Trimmed reads were mapped to hg19/GRCh37 with the mitochondrial genome replaced with the revised Cambridge reference sequence (NC_012920.1). BWA version 0.7.5[40] was used for alignment with non-default parameters *-l 16500*, *-n 0.02* and *-o 2*. Reads were sorted, filtered for a mapping quality (MQ) of 20 or above and PCR duplicates removed using Samtools v0.1.19[41]. Read groups were added and BAM files merged to sample level using Picard Tools v1.101 (http://broadinstitute.github.io/picard/). GenomeAnalysisTK v2.4-7[42] was used to locally realign reads. Two base pairs at both the 5' and 3' ends of reads had their qualities (BQs) reduced to a PHRED score of 2. Where necessary, published ancient data[7,8,11,12,28,35,43–70] was realigned for use in downstream analyses from either unaligned FASTQ (when available) or aligned BAM files following the same parameters described above and filtered in an identical manner.

Radiocarbon Dating and isotope analysis.

Direct radiocarbon dates were obtained for 27 samples from accelerator mass spectrometry facilities at Queen's University Belfast and the University of Oxford. All calibrated dates are taken from CALIB 7.1 after Reimer et al. 2013[71] and reported at two standard deviations (95.4% confidence). The median probabilities (cal BC) have been used for plotting samples chronologically. Stable isotope ratios ($\delta^{13}C$ and $\delta^{15}N$) are also reported for the 27 samples and compared with published stable isotope data from 85 Irish and 81 British samples[8,9,11,14,24,68,72–89] (Fig. 1, Supplementary Table 4). The timeline in Fig. 1 is phased following McLaughlin *et al.* 2016[90].

Molecular sexing and aneuploidy detection with read coverage

Molecular sexing was done following two methods, one previously published[91], and one described as follows. The total number of X chromosome reads was divided by the length of the X chromosome. This value was then divided by the median seen for the same calculation across the autosomal chromosomes. We call this Rx. A value above 0.9 was designated female and below 0.6 as male (Supplementary Table 5). Chromosomal deletions or duplications of sufficient length can be detected by aberrations read coverage for shotgun data. We estimated the chromosomal coverages for 145 shotgun sequenced ancient individuals and 43 samples from the current study (>0.3X mean genome coverage) using Qualimap[92]. To compare chromosomal coverages between samples, we normalised values by the mean autosomal coverage for each genome. An extreme outlier was observed for chromosome 21. To estimate the aberration in read coverage for this sample, we divided its normalised chromosome 21 coverage by the median for this value seen across all samples (Extended Data Fig. 6b).

Mitochondrial analysis

To determine mitochondrial coverages and haplogroups, reads aligned (no MQ filter) to the human reference genome and revised Cambridge mitochondrial reference sequence were realigned to the mitochondrial reference alone and re-processed as described above. Coverages were obtained using Qualimap v2.1.1[92]. Consensus sequences were determined as previously described[45] with Samtools mpileup (-B, -d6 and -Q 30) and vcfutils.pl (vcf2fq)[41]. HaploFind[93] was used to identify defining mutations and assign haplogroups (Supplementary Table 6). Mitochondrial contamination was estimated as previously described[7,62]. Realigned data was not used for these, to avoid the confounding effects of misaligned NUMT sequences. Contamination estimates with and without the inclusion of potential damage sites are given (Supplementary Table 6).

Genotype Calling

As the majority of published ancient genomic data possess sequencing coverages too low for direct diploid genotype calling, two alternative methods were employed - pseudo-diploid genotype calling and genotype imputation. In order to minimize the impact of reference bias previously observed in pseudo-diploidised data[12], a relaxed MQ filter of 20 was applied during data processing. Randomised pseudo-diploid genotypes (BQ>30) were called following previously established methods[7]. Imputation was carried out using Beagle 4.0[94] for 43 individuals from the current study (>0.4X) (Supplementary Data Table 2), and 51 published[7,9,11,28,52,54–56,58,63,64,95] ancient genomes (>0.66X) (Supplementary Data Table 3), following previously published methods[12,35,49,57] with some modifications described below.

Genotype likelihoods for biallelic autosomal SNPs in the 1000 Genomes phase 3 dataset[96] were called using the UnifiedGenotyper tool in GenomeAnalysisTK v2.4-7[42]. These were filtered to add equal likelihoods for missing data and for genotypes which could be the result of post-mortem damage. Samples were merged by chromosome and imputed in 15,000 marker windows using the 1000G phase 3 haplotypic reference panel and genetic map files provided by the BEAGLE website

(http://bochet.gcc.biostat.washington.edu/beagle/). To assess accuracy, imputed genotypes for chromosome 22 of the downsampled Neolithic NE1[35] genome (1X), were compared to direct diploid genotypes from the high coverage version (25X) (Extended Data Fig. 10). Optimal filters of >5% MAF, >99% GP and exclusion of transition sites were subsequently chosen for all downstream analysis. Six individuals, including three from the current study (ANN2, PB754 and PN16), were excluded from downstream analysis due to a high percentage of genotype missingness (>16%) after the imposition of the genotype probability filter. The remaining 88 individuals were combined with published imputed genotypes (filtered identically) from 67 ancient samples[12]. Direct diploid genotype calling was also carried out for high coverage ancient genomes (>10X) at positions in the 1000G Phase 3 variant panel using the HaplotypeCaller tool in GenomeAnalysisTK v4.0[42] with parameter *-mbq 30*. A minimum genotype quality of 30, a minimum depth of coverage of 10X, and a maximum depth of coverage twice that of the sample's mean genomic coverage were required, with a more conservative minimum coverage filter of 15X used for assessment of imputation accuracy.

Pigmentation profiles for high coverage genomes.

We availed of the hIrisPlex-S system to predict hair, skin and eye colour in high coverage ancient samples[97,98]. Diploid genotypes were called at the relevant variant sites and inputted into the hIrisPlex-S online tool (https://hirisplex.erasmusmc.nl). Imputed diploid genotypes (GP > 0.66) were also used for pigmentation prediction across the larger ancient dataset. Results are shown in Supplementary Table 12.

Population genetic analyses.

Detailed descriptions for Y chromosome analysis, ADMIXTURE analysis[99], *D*- and *f*-statistics[100,101] using the AdmixTools package[102], ChromoPainter and fineSTRUCTURE analysis[13], estimations of ROH, inbreeding coefficients and kinship determination with lcMLkin[25] can be found in Supplementary Information sections 2-6. We used smartpca[103,104] to construct the SNP-sharing PCA

in Extended Data Fig. 10, using an identical sample and SNP set as that presented in Fig. 1d, e, with imputed genotypes converted randomly to homozygous to mimic pseudodiploid data. Figures were produced in R[105] using the packages 'ggplot2'[106], 'gplots'[107], 'maps'[108] and 'mapdata'[109], with the 'reshape2'[110] and 'dplyr' [111] packages utilised for data manipulation.

Data availability

Raw FASTQ and aligned BAM files are available through the European Nucleotide Archive under accession number PRJEB36854.

Acknowledgements: We wish to thank the National Museum of Ireland, particularly Mary Cahill, Maeve Sikora and Matthew Seaver for invaluable help in provision of archaeological samples under licence. Also National Museums NI, Marta Mirazón Lahr and the Leverhulme Centre for Human Evolutionary Studies. This work was funded by the Science Foundation Ireland/Health Research Board/Wellcome Trust Biomedical Research Partnership Investigator Award No. 205072 to D.G.B, "Ancient Genomics and the Atlantic Burden". In the early part of the study L.M.C was funded by Irish Research Council Government of Ireland Scholarship Scheme (GOIPG/2013/1219). E.R.J was supported by the Herchel Smith Postdoctoral Fellowship Fund. We thank Rui Martiniano for assisting with an initial sample screening. We acknowledge Trinseq for sequencing support and the DJEI/DES/SFI/HEA Irish Centre for High-End Computing (ICHEC) for the provision of computational facilities. We thank Mikkel Sinding, Pierpaolo Maisano Delser, Kevin Daly, Robert Hensey, Padraig Meehan, Matthew Teasdale for critical reading of the manuscript. We are also grateful to David Reich and two anonymous reviewers for improving the quality of this study.

Contributions: D.G.B and L.M.C designed this study. L.M.C, V.M, A.N and C.C performed laboratory work. L.M.C processed and analysed data with contributions from E.R.J. R.O'M, T.K, A.L, C.J, P.W, E.M, G.R and M.D provided access to samples and supplied archaeological information and interpretation. L.M.C and D.G.B co-wrote the manuscript with input from all authors.

Competing Interests: The authors declare no competing interests.

Materials & Correspondence Requests: Please direct to Lara M. Cassidy (cassidl1@tcd.ie) or Daniel G. Bradley (DBRADLEY@tcd.ie).

460 **Extended References**

461 33. Yang, D. Y., Eng, B., Waye, J. S., Dudar, J. C. & Saunders, S. R. Technical note: improved
462 DNA extraction from ancient bones using silica-based spin columns. *Am. J. Phys. Anthropol.*
463 **105**, 539–543 (1998).
464 34. MacHugh, D. E., Edwards, C. J., Bailey, J. F., Bancroft, D. R. & Bradley, D. G. The extraction
465 and analysis of ancient DNA from bone and teeth: a survey of current methodologies. *Anc.*
466 *Biomol.* **3**, 81–103 (2000).
467 35. Gamba, C. *et al.* Genome flux and stasis in a five millennium transect of European prehistory.
468 *Nat. Commun.* **5**, 5257 (2014).
469 36. Meyer, M. & Kircher, M. Illumina sequencing library preparation for highly multiplexed target
470 capture and sequencing. *Cold Spring Harb. Protoc.* **2010**, db.prot5448 (2010).
471 37. Andrews, S. FastQC: a quality control tool for high throughput sequence data. (2010).
472 38. Martin, M. Cutadapt removes adapter sequences from high-throughput sequencing reads.
473 *EMBnet.journal* **17**, 10–12 (2011)..
474 39. Renaud, G., Stenzel, U. & Kelso, J. leeHom: adaptor trimming and merging for Illumina
475 sequencing reads. *Nucleic Acids Res.* **42**, e141 (2014).
476 40. Li, H. & Durbin, R. Fast and accurate short read alignment with Burrows–Wheeler transform.
477 *Bioinformatics* **25**, 1754–1760 (2009).
478 41. Li, H. *et al.* The Sequence Alignment/Map format and SAMtools. *Bioinformatics* **25**, 2078–
479 2079 (2009).
480 42. McKenna, A. *et al.* The Genome Analysis Toolkit: a MapReduce framework for analyzing
481 next-generation DNA sequencing data. *Genome Res.* **20**, 1297–1303 (2010).
482 43. Keller, A. *et al.* New insights into the Tyrolean Iceman's origin and phenotype as inferred by
483 whole-genome sequencing. *Nat. Commun.* **3**, 698 (2012).
484 44. Olalde, I. *et al.* Derived immune and ancestral pigmentation alleles in a 7,000-year-old
485 Mesolithic European. *Nature* **507**, 225–228 (2014).
486 45. Skoglund, P. *et al.* Genomic diversity and admixture differs for Stone-Age Scandinavian
487 foragers and farmers. *Science* **344**, 747–750 (2014).

46. Allentoft, M. E. *et al.* Population genomics of Bronze Age Eurasia. *Nature* **522**, 167–172 (2015).

47. Günther, T. *et al.* Ancient genomes link early farmers from Atapuerca in Spain to modern-day Basques. *Proc. Natl. Acad. Sci. U. S. A* **38,** 11917-11922 (2015).

48. Haak, W. *et al.* Massive migration from the steppe was a source for Indo-European languages in Europe. *Nature* **522**, 207–211 (2015).

49. Jones, E. R. *et al.* Upper Palaeolithic genomes reveal deep roots of modern Eurasians. *Nat. Commun.* **6**, 8912 (2015).

50. Mathieson, I. *et al.* Genome-wide patterns of selection in 230 ancient Eurasians. *Nature* **528**, 499–503 (2015).

51. Olalde, I. *et al.* A Common Genetic Origin for Early Farmers from Mediterranean Cardial and Central European LBK Cultures. *Mol. Biol. Evol.* (2015).

52. Broushaki, F. *et al.* Early Neolithic genomes from the eastern Fertile Crescent. *Science* **353**, 499–503 (2016).

53. Hofmanová, Z. *et al.* Early farmers from across Europe directly descended from Neolithic Aegeans. *Proc. Natl. Acad. Sci. U. S. A.* **113**, 6886–6891 (2016).

54. Kılınç, G. M. *et al.* The Demographic Development of the First Farmers in Anatolia. *Curr. Biol.* **26**, 2659–2666 (2016).

55. Jones, E. R. *et al.* The Neolithic Transition in the Baltic Was Not Driven by Admixture with Early European Farmers. *Curr. Biol.* **27**, 576–582 (2017).

56. Schiffels, S. *et al.* Iron Age and Anglo-Saxon genomes from East England reveal British migration history. *Nat. Commun.* **7**, 10408 (2016).

57. Martiniano, R. *et al.* Genomic signals of migration and continuity in Britain before the Anglo-Saxons. *Nat. Commun.* **7**, 10326 (2016).

58. González-Fortes, G. *et al.* Paleogenomic Evidence for Multi-generational Mixing between Neolithic Farmers and Mesolithic Hunter-Gatherers in the Lower Danube Basin. *Curr. Biol.* **27**, 1801–1810.e10 (2017).

59. Lipson, M. *et al.* Parallel palaeogenomic transects reveal complex genetic history of early

European farmers. *Nature* **551**, 368–372 (2017).

60. Mathieson, I. *et al.* The genomic history of southeastern Europe. *Nature* **555**, 197–203 (2018).

61. Lazaridis, I. *et al.* Ancient human genomes suggest three ancestral populations for present-day Europeans. *Nature* **513**, 409–413 (2014).

62. Sánchez-Quinto, F. *et al.* Genomic affinities of two 7,000-year-old Iberian hunter-gatherers. *Curr. Biol.* **22**, 1494–1499 (2012).

63. Valdiosera, C. *et al.* Four millennia of Iberian biomolecular prehistory illustrate the impact of prehistoric migrations at the far end of Eurasia. *Proc. Natl. Acad. Sci. U. S. A.* **115**, 3428–3433 (2018).

64. Günther, T. *et al.* Population genomics of Mesolithic Scandinavia: Investigating early postglacial migration routes and high-latitude adaptation. *PLoS Biol.* **16**, e2003703 (2018).

65. Krzewińska, M. et al. Genomic and Strontium Isotope Variation Reveal Immigration Patterns in a Viking Age Town. *Curr. Biol.* **28**, 2730–2738.e10 (2018).

66. Krzewińska, M. et al. Ancient genomes suggest the eastern Pontic-Caspian steppe as the source of western Iron Age nomads. *Sci. Adv.* **4**, eaat4457 (2018).

67. Sikora, M. et al. Ancient genomes show social and reproductive behavior of early Upper Paleolithic foragers. *Science* **358**, 659–662 (2017).

68. Scheib, C. L. et al. East Anglian early Neolithic monument burial linked to contemporary Megaliths. *Ann. Hum. Biol.* **46**, 145–149 (2019).

69. Saag, L. et al. Extensive Farming in Estonia Started through a Sex-Biased Migration from the Steppe. *Curr. Biol.* **27**, 2185–2193.e6 (2017).

70. Rodríguez-Varela, R. et al. Genomic Analyses of Pre-European Conquest Human Remains from the Canary Islands Reveal Close Affinity to Modern North Africans. *Curr. Biol.* **28**, 1677–1679 (2018).

71. Reimer, P. J. *et al.* IntCal13 and Marine13 Radiocarbon Age Calibration Curves 0–50,000 Years cal BP. *Radiocarbon* **55**, 1869–1887 (2013).

72. Eogan, G. Excavations at Knowth: The Passage Tomb Archaeology of the Great Mound at Knowth. in (Royal Irish Academy, 2017).

73. Hamilton, J. & Hedges, R. E. M. Carbon and nitrogen stable isotope values of animals and humans from causewayed enclosures: *Gathering Time* (eds. Whittle, A., Healy, F. & Bayliss, A.) 670–681 (Oxbow Books, 2011).

74. Hutchison, M., Curtis, N. & Kidd, R. The Knowe of Rowiegar, Rousay, Orkney. *Proceedings of the Society of Antiquaries of Scotland* **145**, 41–89 (2015).

75. Kador, T., Fibiger, L., Cooney, G. & Fullagar, P. Movement and diet in early Irish prehistory: First evidence from multi-isotope analysis. *Journal of Irish Archaeology* **23**, 83–96 (2015).

76. Schulting, R. On the northwestern fringes: earlier Neolithic subsistence in Britain and Ireland as seen through faunal remains and stable isotopes: *The origins and spread of domestic animals in southwest Asia and Europe* (eds. Colledge, S. *et al.*) 313–338 (2013).

77. Schulting, R. J., Murphy, E., Jones, C. & Warren, G. New dates from the north and a proposed chronology for Irish court tombs. *Proc. R. Ir. Acad. C Archaeol. Celt. Stud. Hist. Linguist. Lit.* **112C**, 1–60 (2012).

78. Wysocki, M. *et al.* Dates, Diet, and Dismemberment: Evidence from the Coldrum Megalithic Monument, Kent. *Proceedings of the Prehistoric Society* **79**, 61–90 (2013).

79. Wysocki, M., Bayliss, A. & Whittle, A. Serious Mortality: the Date of the Fussell's Lodge Long Barrow. *Cambridge Archaeological Journal* **17**, 65–84 (2007).

80. Whittle, A. *et al.* Parc le Breos Cwm Transepted Long Cairn, Gower, West Glamorgan: Date, Contents, and Context. *Proceedings of the Prehistoric Society* **64**, 139–182 (1998).

81. Whittle, A., Bayliss, A. & Wysocki, M. Once in a Lifetime: the Date of the Wayland's Smithy Long Barrow. *Cambridge Archaeological Journal* **17**, 103–121 (2007).

82. Bayliss, A., Whittle, A. & Wysocki, M. Talking About My Generation: the Date of the West Kennet Long Barrow. *Cambridge Archaeological Journal* **17**, 85–101 (2007).

83. Brindley, A. L., Lanting, J. N. & van der Plicht, J. Radiocarbon-dated samples from the Mound of the Hostages: *Duma na nGial: The Mound of the Hostages, Tara* (ed. O'Sullivan, M.) 281–296 (Wordwell, 2005).

84. Schulting, R. J., Chapman, M. & Chapman, E. J. AMS 14C dating and stable isotope (carbon, nitrogen) analysis of an earlier Neolithic human skeletal assemblage from hay wood cave,

572 Mendip, Somerset. *Proc. Univ. Bristol Spelaeol. Soc.* **26**, 9–26 (2013).
573 85. Schulting, R. et al. Mesolithic and Neolithic Human Remains from Foxhole Cave, Gower,
574 South Wales. *The Antiquaries Journa*l **93**, 1–23 (2013).
575 86. Sheridan, J. A., Schulting, R., Quinnell, H. & Taylor, R. Revisiting a small passage tomb at
576 Broadsands, Devon. *Proceedings of the Devon Archaeological Society* **66**, 1–26 (2008).
577 87. Schulting, R. J. & Richards, M. P. Finding the coastal Mesolithic in southwest Britain: AMS
578 dates and stable isotope results on human remains from Caldey Island, south Wales. *Antiquity*
579 **76**, 1011–1025 (2002).
580 88. Stevens, R. E., Lightfoot, E., Allen, T. & Hedges, R. E. M. Palaeodiet at Eton College Rowing
581 Course, Buckinghamshire: isotopic changes in human diet in the Neolithic, Bronze Age, Iron
582 Age and Roman periods throughout the British Isles. *Archaeological and Anthropological*
583 *Sciences* **4**, 167–184 (2012).
584 89. Chamberlain, A. T. & Witkin, A. V. A Neolithic cairn at Whitwell, Derbyshire. *Derbyshire*
585 *Archaeol. J.* **131**, 1–131 (2011).
586 90. McLaughlin, T. R., Whitehouse, N. J. & Schulting, R. J. The Changing Face of Neolithic and
587 Bronze Age Ireland: A Big Data Approach to the Settlement and Burial Records .*Journal of*
588 *World Prehistory*, **29**, 117–153 (2016).
589 91. Skoglund, P., Storå, J., Götherström, A. & Jakobsson, M. Accurate sex identification of ancient
590 human remains using DNA shotgun sequencing. *J. Archaeol. Sci.* **40**, 4477–4482 (2013).
591 92. Okonechnikov, K., Conesa, A. & García-Alcalde, F. Qualimap 2: advanced multi-sample
592 quality control for high-throughput sequencing data. *Bioinformatics* **32,** 292-294 (2015).
593 93. Vianello, D. et al. HAPLOFIND: a new method for high-throughput mtDNA haplogroup
594 assignment. *Hum. Mutat.* **34**, 1189–1194 (2013).
595 94. Browning, S. R. & Browning, B. L. Rapid and accurate haplotype phasing and missing-data
596 inference for whole-genome association studies by use of localized haplotype clustering. *Am. J.*
597 *Hum. Genet*. **81**, 1084–1097 (2007).
598 95. Gallego-Llorente, M. et al. The genetics of an early Neolithic pastoralist from the Zagros, Iran.
599 *Sci. Rep.* **6**, 31326 (2016).

600 96. 1000 Genomes Project Consortium et al. A global reference for human genetic variation.
601 *Nature* **526**, 68–74 (2015).
602 97. Walsh, S. et al. The HIrisPlex system for simultaneous prediction of hair and eye colour from
603 DNA. *Forensic Sci. Int. Genet.* **7**, 98–115 (2013).
604 98. Chaitanya, L. et al. The HIrisPlex-S system for eye, hair and skin colour prediction from DNA:
605 Introduction and forensic developmental validation. *Forensic Sci. Int. Genet.* **35**, 123–135
606 (2018).
607 99. Alexander, D. H., Novembre, J. & Lange, K. Fast model-based estimation of ancestry in
608 unrelated individuals. *Genome Res.* **19**, 1655–1664 (2009).
609 100. Green, R. E. et al. A draft sequence of the Neandertal genome. Science 328, 710–722 (2010).
610 101. Reich, D., Thangaraj, K., Patterson, N., Price, A. L. & Singh, L. Reconstructing Indian
611 population history. *Nature* **461**, 489–494 (2009).
612 102. Patterson, N. et al. Ancient admixture in human history. *Genetics* **192**, 1065–1093 (2012).
613 103. Patterson, N., Price, A. L. & Reich, D. Population structure and eigenanalysis. *PLoS Genet.* **2**,
614 e190 (2006).
615 104. Price, A. L. et al. Principal components analysis corrects for stratification in genome-wide
616 association studies. *Nat. Genet.* **38**, 904–909 (2006).
617 105. R Core Team. *R: A language and environment for statistical computing*. (R Foundation for
618 Statistical Computing, 2015).
619 106. Wickham, H. *ggplot2: elegant graphics for data analysis.* (Springer, 2016).
620 107. Warnes, G.R. *et al.* gplots: Various R programming tools for plotting data. R package version
621 3.0.1. http://CRAN.R-project.org/package=gplots (2016).
622 108. Becker, R. A., Wilks, A. R., Brownrigg, R., Minka, T. P. & Deckmyn, A. maps: Draw
623 Geographical Maps. R package version 3.1.0. http://CRAN.R-project.org/package=maps
624 (2016).
625 109. Becker, R. A., Brownrigg, R. & Wilks, A. R. mapdata: Extra Map Databases. R package
626 version 2.2-6. http://CRAN.R–project.org/package=mapdata (2016).
627 110. Wickham, H. Reshaping Data with the reshape Package. *Journal of Statistical Software.* **21**, 1-

20 (2007).

111. Wickham, H., François, R., Henry, L., & Müller, K. dplyr: A grammar of data manipulation. R package version 0.7.6. http://CRAN.R–project.org/package=dplyr (2018).

Extended Data Fig. 1. Genomic Affinities of the Irish Neolithic. a, ADMIXTURE plots (K=14) for ancient Irish and British populations (first row), other ancient Eurasians (second and third rows) and global modern populations (fourth row). For components that reach their maximums in modern populations, the five individuals with highest values were selected for representation. If the majority of these come from a single population the block is labelled as such, otherwise it is labelled using the general geographic region from which these individuals originate. Three components reach their maximum in ancient populations and we label these *European_HG* (Red), *Early_Farmer* (Orange) and *Steppe* (teal). **b,** Box plot (Tukey method) showing the distribution of the *European_HG* component among British and Irish Neolithic shotgun-sequenced individuals (n=50). **c,** Normalised haplotypic length contributions, estimated with ChromoPainter, from Early Neolithic populations to later Neolithic and Chalcolithic individuals. The top two donors are outlined in black for each individual. Given the unsupervised nature of the analysis, regional differences in overall haplotypic donation levels should be ignored, as larger populations have more opportunity for within group painting.

Extended Data Fig. 2. Haplotypic structure among ancient populations. a, ChromoPainter PCA of diverse ancient genomes (n=149) generated using the output matrix of haplotypic lengths. Colour and shape key for Irish samples follows Fig. 1. **b,** fineSTRUCTURE dendrogram derived from the same matrix with the passage tomb cluster highlighted.

Extended Data Fig. 3. Inferring the relationship between NG10's parents. a, Whole genome plot of heterozygosity in NG10, revealing extreme ROH. **b,** Nine matings (coloured lines) that can lead to an inbreeding coefficient of 25%. **c,** Number and average lengths of homozygous-by-descent (HBD) segments for each of these simulated scenarios (500 iterations) and the same values observed for NG10 genome. Box plots follow the Tukey method. Scenarios in **i** and **ii** best fit the HBD distribution of NG10, with **ii** being less parsimonious when anthropological and biological factors are taken into consideration.

Extended Data Fig. 4. Levels of inbreeding through time in ancient populations. Inbreeding coefficients for imputed ancient samples estimated by measuring the proportion of the genome that is homozygous-by-descent (HBD). Boxplots follow Tukey's method. Individuals are binned according to archaeological period - UP-MS: Upper Palaeolithic to Mesolithic (n=24), EN: Early Neolithic (n=13), MN-CA: Middle Neolithic-Chalcolithic (n=69), BA: European Bronze Age (n=12), IA: IA-MA: Iron Age to Medieval (n=21), Steppe CA-BA (n=14). Outliers of note are labelled. The inferred degrees of relatedness between an individual's parents are marked.

Extended Data Fig. 5. Detecting recent shared ancestry between pairs of British and Irish Neolithic samples. a, lcMLkin[29] kinship coefficients between pairs of Irish and British Neolithic samples, jittered by a height of 0.00018 and width of 0.00036 for visualisation. Optimised duplicate tests are linked by dotted lines. Several standalone values are also shown (italics), where one duplicate did not meet the threshold of overlapping sites (>20,000). The MB6 and car004 pairing (19,850 sites) is shown as a translucent point. An inset is shown for lower values of pi-HAT. Pairs over 5σ from the mean pi-HAT and K_0 for panel *ii* (marked with line) are highlighted using the same colour and shape key as Fig. 1. Combined symbols are used for inter-site pairs. **b,** Total haplotypic lengths donated between all pairs (n=2162) of British and Irish samples from the ChromoPainter analysis of diverse ancient samples (Extended Data Fig. 2). Outlying pairs (4σ above the mean) are labelled. **c,** Outgroup f_3-statistics measuring shared drift between pairs (n=2236) of Irish and British Neolithic samples

(>25,000 informative sites). **d,** Total haplotypic lengths donated between all pairs of 'passage cluster' (pink; n=42) and 'British-Irish cluster' (grey; n=1190) samples from the ChromoPainter analysis of Atlantic Neolithic genomes (Fig. 1d, e).

Extended Data Fig. 6. Regional-scale diversity in the Irish Neolithic. a, Nitrogen stable isotope values, an indicator of trophic level, plotted across time for samples from the neighbouring sites of Poulnabrone (blue) and Parknabinnia (yellow). For male samples, the Y chromosome haplogroup is given. Distant kinship connections are marked with a dotted line, while a closer (~4th degree) relationship is highlighted with a solid line. **b,** Boxplot (Tukey method) of normalised read coverage aligning to chromosome 21 for shotgun sequenced ancient samples (n=188), with a single trisomy outlier infant.

Extended Data Fig. 7. Subclade distributions of Y chromosome haplogroup I2a1 in Ireland, Britain and Europe from the Mesolithic to Bronze Age. a, Y haplogroups observed for Neolithic individuals (jittered) in Britain and Ireland. Shape indicates the approximate time period within the Neolithic based on McLaughlin *et al.* 2016[90], while colour indicates haplogroup and follows the same keys as in **b, c** and **d**. Approximately 94% of the British-Irish Neolithic sample belong to haplogroups I2a1b1 (45%), I2a1a1 (14%) and I2a1a2 (35%). Incidences (jittered) of these haplogroups in European individuals from the Mesolithic to Bronze Age are shown in **b** (I2a1b1), **c** (I2a1a1) and **d** (I2a1a2). Haplogroup colour keys are shown with respect to phylogenetic placement, with those observed within Britain and Ireland in bold. European individuals who share an identical set of haplotypic mutations (for sites covered) to an Irish Neolithic individual are highlighted with a black outline in **c** (I2a1a1) and **d** (I2a1a2)**.**

Extended Data Fig. 8. Geographic and genomic distributions of northwestern European HG (NWHG) ancestry among British and Irish Neolithic individuals. a, Geographical distribution of NWHG introgression in Britain and Ireland across 103 Neolithic samples. Box plot (Tukey method) highlights four outliers, three from the Early to Middle Neolithic of Argyll and one from Ireland -

712 Parknabinnia675 (PB675). The next highest value is also from Parknabinnia, PB754. **b,** The same *D*-
713 statistic run on separate chromosomes for individuals of sufficient coverage (n=86). Outlying
714 individuals are marked for each chromosome. Irish outliers follow the same shape and colour key as
715 in Fig. 1 and outliers who are also outliers in the box plot in **a** are marked in bold. **c,** Box plot (Tukey
716 method; n=86) of sample standard deviations across the chromosomes for the same *D*-statistic. Four
717 outliers with high variance across the chromosomes are marked, including three samples from
718 Parknabinnia, two of whom are also top hits in **a**. **d,** Haplotypic affinities of imputed Irish and British
719 Neolithic individuals (n=47) to Irish HGs, relative to other NWHGs (Bichon, Loschbour and
720 CheddarMan). Colour and shape key follows Fig. 1. The outlying individual PB675 shows a
721 preference for Irish HG haplotypes in all measures. Regression lines are shown with 95% confidence
722 interval shaded (sample size=47). PB675 shows a higher than expected number of Irish HG
723 haplotypes (panel i), has the highest overall HG haplotypic length contribution, with a ratio skewed
724 towards Irish HG (panel ii). and displays the longest average length of Irish HG haplotype chunks
725 (panel iii)

726 **Extended Data Fig. 9. SNP-sharing analyses of autosomal structure in Atlantic Neolithic**
727 **populations. a,** PCA created using an identical sample (n=57) and SNP set (~488k sites;
728 pseudiploidised) as that presented in Fig. 1d, e. **b,** Outgroup f_3-statistics for all combinations of
729 samples in **a,** using a reduced SNP set (~270k sites; pseudiploidised). Results are presented in a
730 heatmap and corresponding dendrogram.

731

732 **Extended Data Fig. 10. Imputation accuracies for chromosome 22 of the high coverage NE1**
733 **genome downsampled to 1X.** The levels of accuracy seen across all SNPs (solid line; n=204,316 for
734 no MAF filter and GP 80) is compared to that seen for transversions only (dashed line; n=62,374 for
735 no MAF filter and GP 80). Accuracies at different genotype probability (GP) thresholds and minor
736 allele frequency (MAF) filters are shown for the three different genotype categories. MAF filters are
737 based on overall frequency in the 1000 Genomes phase 3 dataset.

738

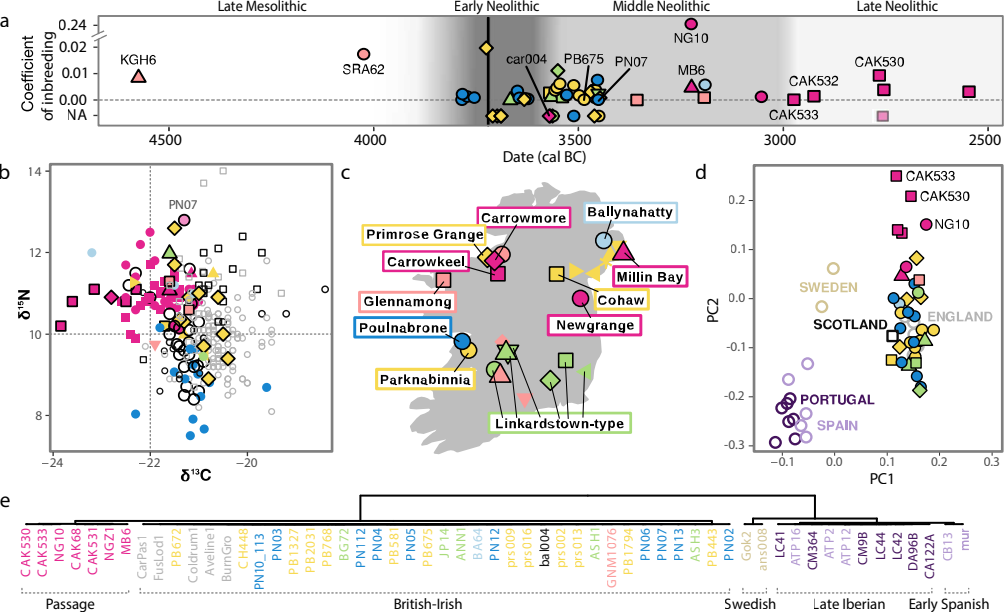
a
Late Mesolithic
Early Neolithic
Middle Neolithic
Late Neolithic
Coefficient of inbreeding
0.24
0.02
0.01
0.00
NA
KGH6
SRA62
car004
PB675
PN07
NG10
MB6
CAK532
CAK530
CAK533
4500
4000
3500
3000
2500
Date (cal BC)
b
PN07
δ15N
δ13C
c
Carrowmore
Ballynahatty
Primrose Grange
Carrowkeel
Millin Bay
Glennamong
Cohaw
Poulnabrone
Newgrange
Parknabinnia
Linkardstown-type
d
CAK533
CAK530
NG10
SWEDEN
SCOTLAND
ENGLAND
PORTUGAL
SPAIN
PC1
PC2
e
CAK530
CAK533
NG10
CAK68
CAK531
NGZ1
MB6
CarPas1
FusLod1
PB672
Coldrum1
Aveline1
BurnGro
CH448
PN10_113
PN03
PB1327
PB2033
PB768
BG72
PN112
PN04
PB588
PN05
PB675
JP14
ANN1
BA64
PN12
prs009
prs016
bal004
prs002
prs015
ASH1
GNM1076
PB1794
PN06
PN07
PN13
ASH3
PB443
PN02
Gok2
ans008
LC41
ATP16
CM364
ATP2
ATP12
CM98
LC44
LC42
DA968
CA122A
CB13
mur
Passage
British-Irish
Swedish
Late Iberian
Early Spanish

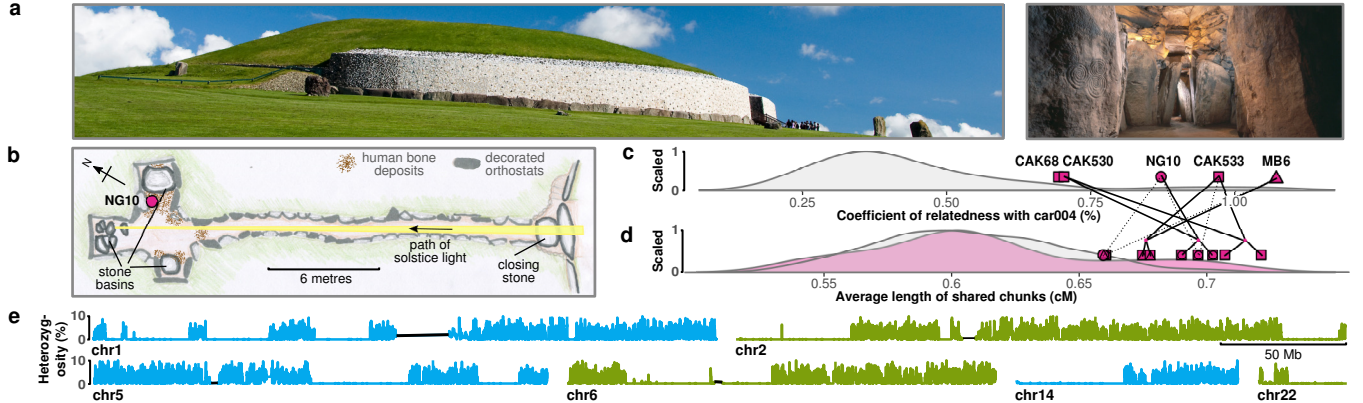
a
b
N
NG10
human bone deposits
decorated orthostats
path of solstice light
stone basins
6 metres
closing stone
c
Scaled
1
0
CAK68 CAK530
NG10
CAK533
MB6
0.25
0.50
0.75
1.00
Coefficient of relatedness with car004 (%)
d
Scaled
1
0
0.55
0.6
0.65
0.7
Average length of shared chunks (cM)
e
Heterozygosity (%)
10
0
chr1
chr2
50 Mb
chr5
chr6
chr14
chr22

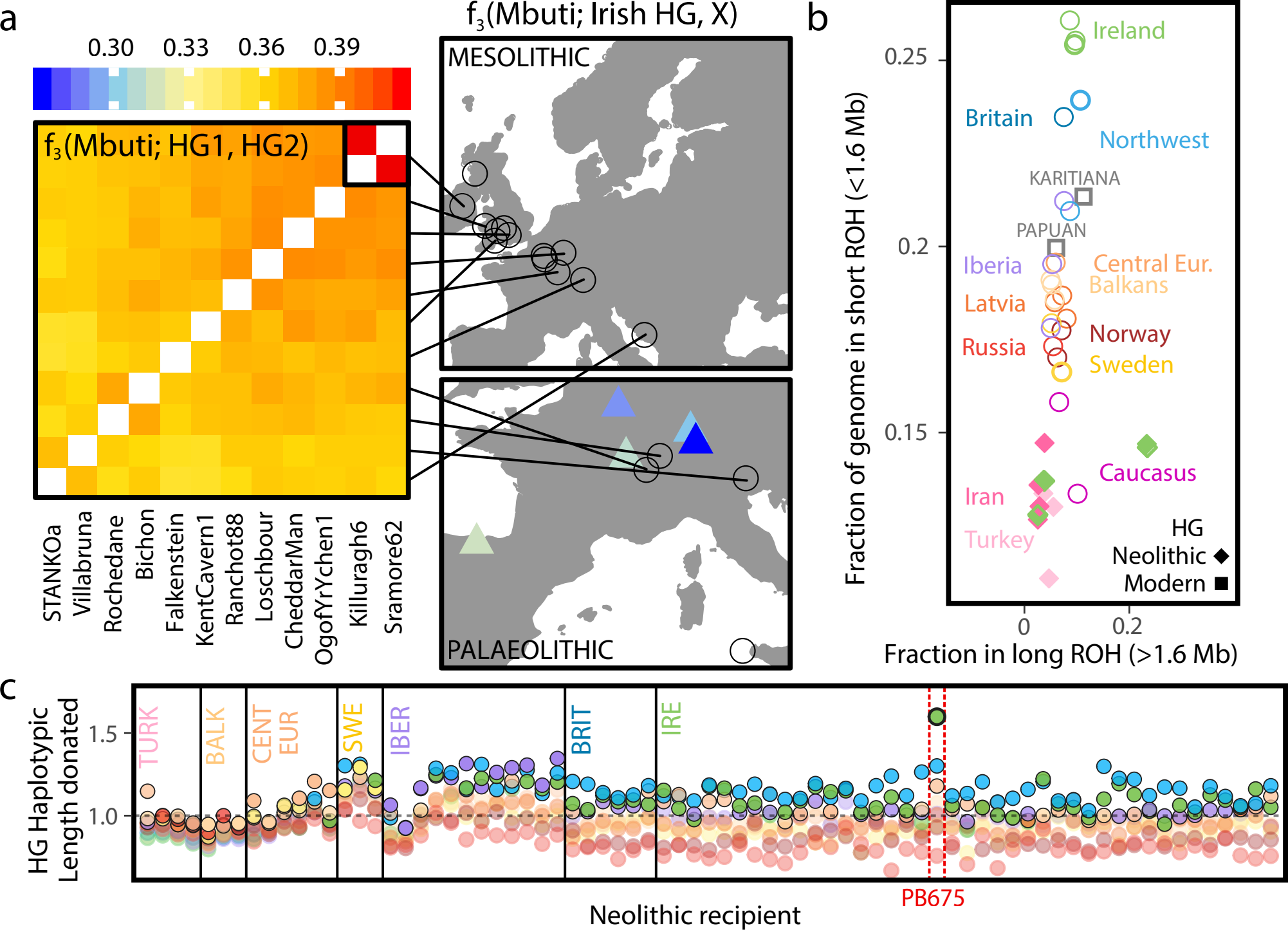
a
0.30
0.33
0.36
0.39
f3(Mbuti; HG1, HG2)
STANKOa
Villabruna
Rochedane
Bichon
Falkenstein
KentCavern1
Ranchot88
Loschbour
CheddarMan
OgofYrYchen1
Killuragh6
Sramore62
f3(Mbuti; Irish HG, X)
MESOLITHIC
PALAEOLITHIC
b
Fraction of genome in short ROH (<1.6 Mb)
0.25
0.2
0.15
Ireland
Britain
Northwest
KARITIANA
PAPUAN
Iberia
Central Eur.
Balkans
Latvia
Norway
Russia
Sweden
Caucasus
Iran
Turkey
HG
Neolithic
Modern
0
0.2
Fraction in long ROH (>1.6 Mb)
c
HG Haplotypic Length donated
1.5
1.0
TURK
BALK
CENT EUR
SWE
IBER
BRIT
IRE
PB675
Neolithic recipient